Volume 49
Number 48
28 December 2025
Pages 20771–21114

NJC

New Journal of Chemistry

A journal for new directions in chemistry

rsc.li/njc

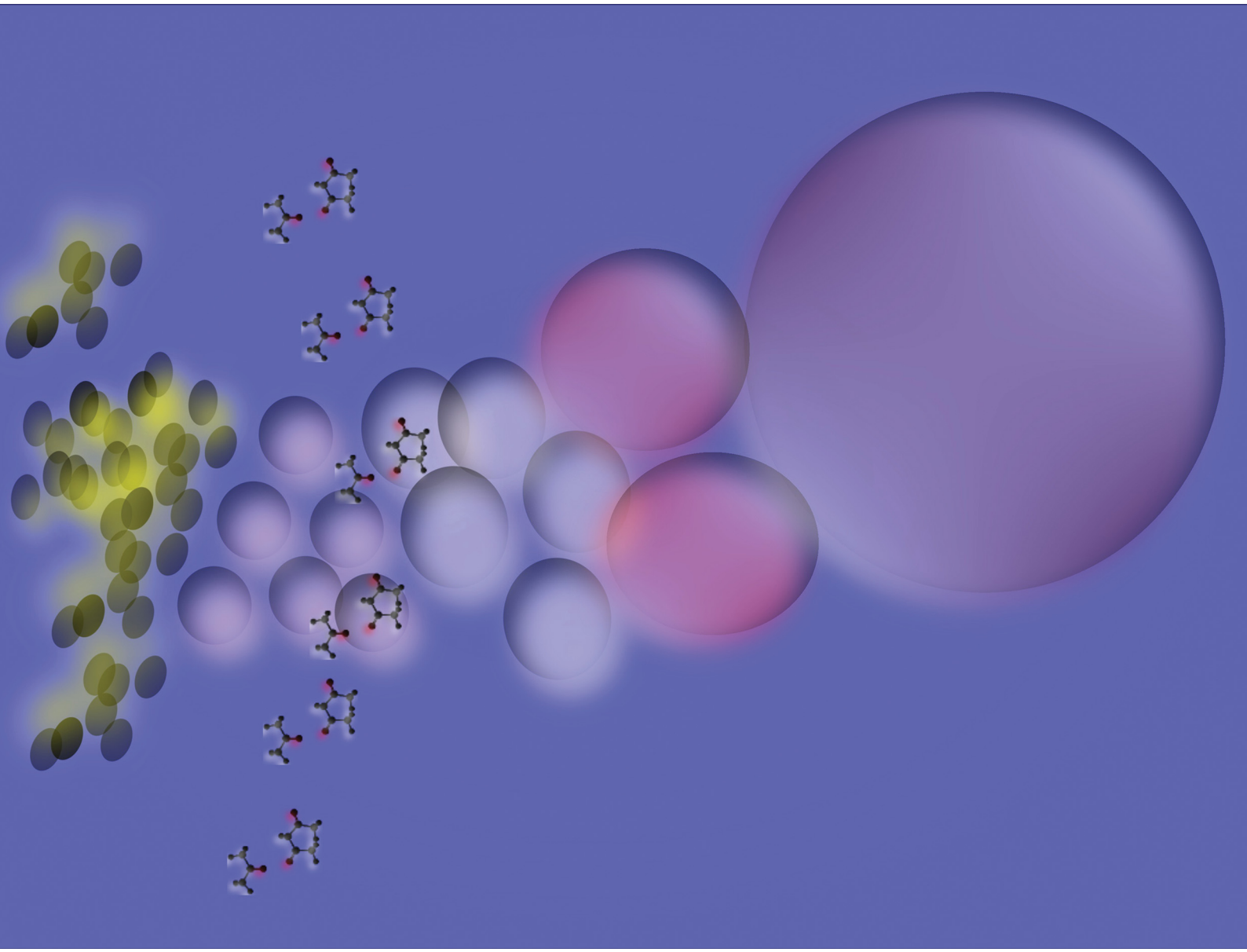

ISSN 1144-0546

ROYAL SOCIETY OF CHEMISTRY

PAPER

Vian Mahmood Saleh *et al.*

Novel synthesis and SPR characterization of gold nanoparticles

cnrs

NJC

ROYAL SOCIETY OF CHEMISTRY

PAPER

View Article Online
View Journal | View Issue

Cite this: *New J. Chem.*, 2025, **49**, 20799

Novel synthesis and SPR characterization of gold nanoparticles

Vian Mahmood Saleh,*[ab] Christopher Zaleski,[a] Elena Piletska[a] and Sergey A. Piletsky[a]

Received 12th August 2025,
Accepted 22nd October 2025

DOI: 10.1039/d5nj03249k

rsc.li/njc

A novel protocol for the synthesis of gold nanoparticles (AuNPs) is presented, utilizing $HAuCl_4$ and a 1 : 2 acetone–acetylacetone mixture as the reducing agent. Nanoparticle size was regulated by reagent concentration. Characterization confirmed spherical AuNPs with an LSPR peak at 521 nm and average sizes of 14.7 nm (TEM) and 23.7 nm (DLS), indicating biomedical relevance.

1. Introduction

The discovery of colloidal gold dates back to the pioneering work of Michael Faraday in the 1850 s, when he reduced sodium chloroaurate in suspension and observed the distinctive optical properties of the resulting colloidal dispersion, later known as "Faraday gold".[1–3] Faraday also reported the Faraday–Tyndall effect, where incident light was scattered by fine gold particles suspended in liquid, thereby laying the foundation for modern nanoscience and nanotechnology.[1–3] Since then, gold nanoparticles (AuNPs) have become among the most widely studied nanomaterials, particularly for biomedical applications, due to their favourable physicochemical features including facile synthesis, straightforward surface modification, high surface-to-volume ratio, size-dependent optical properties, biocompatibility, and relatively low toxicity.[4,5] Wang *et al.* (2024) demonstrated that nanostructured platforms can achieve highly selective detection, reinforcing the diagnostic potential of SPR-active AuNPs. Such findings underscore the importance of refining AuNP synthesis methods to obtain high stability, uniformity, and tunable optical properties for analytical and biomedical applications.[6] Unlike bulk gold, the properties and colour diversity of AuNPs are strongly dictated by particle size and morphology, making them attractive for a variety of technological and biological uses.[4,5] The unique optical, chemical, and physical characteristics of AuNPs have enabled their integration into diverse fields, spanning optical imaging, cancer therapy, biosensing, medical diagnostics, and drug delivery[7–9] (Fig. 1). Nanoparticle synthesis strategies are generally classified as top-down or bottom-up. The top-down approach involves breaking down bulk materials into nanoscale structures, whereas the bottom-up approach assembles atoms or molecules to build nanostructures.[10–13] A wide range of physical, chemical, and biological routes have been employed within these categories, as depicted in (Table S1).[14] Chemical approaches are attractive for their simplicity and scalability though they frequently rely on hazardous reagents. By contrast, biological syntheses harness metabolites such as proteins, fatty acids, and phenolic compounds from microbial or plant sources, enabling eco-friendly bio reduction and improved nanoparticle stability, albeit often with reduced control over particle size.[5,14,15] Biosynthesised AuNPs have been applied successfully in antibacterial, anticancer, anti-inflammatory, and antioxidant contexts,[15] yet reproducibility and tunability remain challenges. Chemical syntheses, on the other hand, afford precise size control but can yield toxic by-products detrimental to environmental and human health.[16,17]

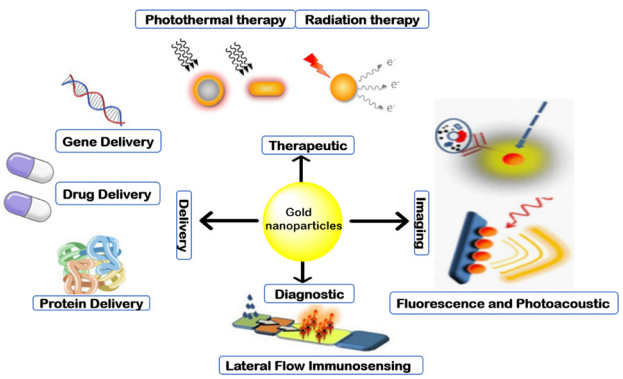

Fig. 1 A diagram representing the diverse applications of AuNPs.

[a] *Leicester Biotechnology Groups, School of Chemistry, College of Science and Engineering, University of Leicester, University Rd, LE1 7RH Leicester, UK. E-mail: vmss2@leicester.ac.uk, ep219@leicester.ac.uk*
[b] *Department of Chemistry, College of Science, University of Sulaymaniyah, 46001 Sulaymaniyah, Iraq*

Among chemical methods, citrate reduction (Turkevich/Frens) is widely used but requires boiling conditions and relatively long reaction times for size control.[18,19] Sodium borohydride, a stronger reductant, rapidly produces ultrasmall AuNPs but generates highly unstable colloids and poses safety concerns due to hydrogen release.[20] Ketone-based reductions, particularly those employing acetylacetone or Au(III)–β-diketonate intermediates, offer alternatives but typically require complex precursors, light activation, or elevated temperatures.[21] Thus, while many reductants exist, a gap persists for a simple, rapid, aqueous synthesis at room temperature that (i) yields stable colloids in the 10–30 nm range, (ii) permits size tunability through straightforward reagent control, and (iii) is inherently compatible with downstream functionalisation techniques such as silanization, Au-thiol coupling, and molecular imprinting.[22] In diagnostics, gold nanoparticles (AuNPs) have been extensively utilized in colorimetric assays, lateral flow tests, biosensors, and optical imaging, owing to their size- and shape-dependent optical properties.[23] Qian *et al.* (2025) highlighted the importance of precise nanostructure control for biomedical applications, demonstrating that optimized physicochemical parameters can significantly enhance nanoparticle based diagnostics.[24] Lei *et al.* (2025) and Sun *et al.* (2025) have shown that integrating advanced physical or optical tools such as magnetic field based generators and cavity ring-down spectroscopy (CRDS) can significantly improve real-time analyte detection and nanoparticle control, illustrating the potential of AuNPs in dynamic diagnostic monitoring.[25,26] These advances align closely with the goals of the present work, which focuses on producing stable, reproducible AuNPs with tunable optical properties suitable for sensing applications. The relationship between nanoparticle morphology and optical response is critical. Gao, Sun, and Du (2025) demonstrated that controlled nanostructure growth profoundly influences surface plasmon resonance behaviour, highlighting the importance of morphology in determining sensitivity and specificity in optical sensing.[27] Similarly, Gao *et al.* (2025) developed luminescent polypeptide-based nanoparticles exhibiting tumor-selective responses, illustrating how tailored nanostructure design can be harnessed for biomedical diagnostics.[28] In another study, Fagonia arabica extract-stabilized AuNPs were reported to possess high selectivity toward Cd^{2+} detection, along with photocatalytic and antibacterial properties, underscoring the multifunctional potential of gold nanostructures.[29] These studies collectively reinforce the broader impact of nanomaterial design in biosensing and therapeutic systems. Electrochemical and optical sensing platforms continue to evolve in sensitivity and selectivity through the integration of metallic nanomaterials. For example, a sandwich electrochemical immunosensor based on antibody-functionalized silver nanoparticles was developed for detecting the dengue biomarker protein NS1, demonstrating the adaptability of nanoparticle-based platforms for disease diagnostics.[30] Such examples illustrate how nanomaterials can be engineered for target-specific recognition and detection.

Common chemical synthesis methods, such as citrate reduction and sodium borohydride reduction, have been widely employed to produce AuNPs for these applications due to their relatively predictable size control.[31] Chemical synthesis, despite its simplicity and scalability, often relies on potentially hazardous reagents and requires separate functionalization steps to impart specific biological recognition capabilities.[32,33] This process can be time-consuming and environmentally taxing, particularly when compared to biosynthetic or enzymatic approaches. Biological synthesis approaches, while environmentally friendly and biocompatible, typically yield polydisperse nanoparticles with less reproducible optical properties, limiting their diagnostic performance.[34] Consequently, there remains a need for a synthesis route that is simple, rapid, and produces stable, tunable AuNPs compatible with diagnostic platforms. To address this gap, we report a novel one-pot protocol based on a defined 1 : 2 acetone : acetylacetone reducing mixture. This approach reduces $HAuCl_4$ directly in aqueous solution under ambient conditions, producing stable AuNPs within one minute without the need for elevated temperatures or external activation.[21,22] By adjusting the concentration of the reducing mixture, particle size can be tuned reproducibly, yielding uniform spherical nanoparticles of ~15–25 nm with narrow size distributions.[21] Compared to citrate and borohydride reductions, this acetone–acetylacetone system is milder, safer, and generates colloids ideally suited for integration into molecularly imprinted polymers and optical sensing platforms.[20–22] In light of recent advancements, this study introduces a novel, rapid, and environmentally benign chemical approach offering an efficient and scalable route for the synthesis of gold nanoparticles that meet the practical requirements of nanotechnology, biosensing, and diagnostic applications.

2. Experimental

2.1. Experimental procedure for the synthesis of gold nanoparticles

Gold nanoparticles were synthesized using a novel method (Fig. S1A). Deionised water (5 mL) was purged with N_2 for 10 minutes, followed by the addition of 60 μL $HAuCl_4$ (0.7 mg mL^{-1}, 30 mM). After one minute of mixing, varying volumes (0.125–1 mL) of a reducing agent (4.5 M acetone and 6.47 M acetylacetone, mixed 1 : 2) were introduced. Nitrogen purging continued until the solution turned pink-purple within a minute, confirming nanoparticle formation (Fig. S1B). Full details about the materials are provided in the SI.

2.2. Comprehensive characterization of synthesized gold nanoparticles

Gold nanoparticles were thoroughly characterized due to their dependence on size, surface texture, and shape, with their formation visually confirmed by a distinct colour change from light yellow to red. Size and morphology were analyzed using dynamic light scattering (DLS), localized surface plasmon resonance (LSPR), Transmission electron microscopy (TEM), and Fourier transform infrared spectroscopy (FTIR), as detailed in the SI. All measurements were performed in triplicate (n = 3).

For TEM, at least 200 particles per replicate were measured using ImageJ to calculate the average diameter, while DLS and PDI analyses were conducted on independent AuNP batches. Reported error margins (±) correspond to standard deviation (SD). This approach ensures reproducibility and provides a reliable assessment of nanoparticle size distribution and dispersity.[35,36]

3. Results and discussion

3.1. Synthesis of gold nanoparticles

AuNPs are nanoparticles synthesized *via* the reduction method as shown in (Scheme 1). Acetylacetone, which is alternatively referred to as 2,4-pentanedione, has been employed as a reducing agent in certain methodologies for the synthesis of gold nanoparticles.[21] The reducing action of acetylacetone is facilitated by the carbonyl groups, which donate electrons to the reduction of gold ions (Au^{+3} to Au^{0}). Additionally, acetone weakly reduces the metal ions, while it can help prevent premature aggregation of nanoparticles by maintaining the nanoparticles dispersed in the solution. This is particularly important for achieving smaller and more uniform nanoparticles. During this study, a variety of reducing agents were evaluated for the synthesis of gold nanoparticles (AuNPs), including cyclohexanone, ascorbic acid, triacetin, benzophenone, dimethoxy acetophenone, urea, uric acid, glucose, fructose, uridine, an acetone/hydrogen peroxide mixture, acetone, and acetylacetone. Using acetone alone leads to partial reduction of Au^{3+} ions, resulting in rapid nucleation and uncontrolled growth of particles, which causes clustering and precipitation with limited stability. This observation aligns with our experimental results, where AuNPs synthesized using only acetone displayed visible aggregation and sedimentation within hours of preparation, as depicted in (Fig. S2). Conversely, other ketones such as cyclohexanone proved unsuitable due to acid-catalyzed polymerization during synthesis, leading to unwanted by-products and unstable colloidal suspensions. These results emphasize the need for careful selection of reducing agents to ensure controlled particle nucleation and long-term stability. Prompted further investigation of the two most effective reducing agents, which were acetone and acetylacetone. As a result of this, we investigated acetone and acetylacetone, the optimized mixture of acetone and acetylacetone in a 1 : 2 molar ratio provides a balance between reduction potential and complexation ability. The enol form of acetylacetone stabilizes Au^{3+} intermediates *via* chelation, moderating the reduction kinetics and promoting the formation of uniformly dispersed nanoparticles. Deviations from this optimal ratio (*e.g.*, 1 : 1 or 2 : 1) led to aggregation over time, demonstrating the crucial role of precise stoichiometric control in maintaining colloidal stability and reproducibility, as shown in Fig. S3. The concentration of the acetone/acetylacetone mixture significantly influences the reduction rate of gold ions during the synthesis of gold nanoparticles (AuNPs). Mostly, an increase in the concentration of the reducing agent results in a more rapid progression of the kinetics of the reduction reaction, which ultimately causes the particle size to decrease.

3.2. Morphological and optical characterizations

Gold nanoparticles exhibit localized surface plasmon resonance, which results in a strong absorbance band in the visible region (500–600 nm). The spectra obtained are shown in Fig. 2. As expected, AuNPs exhibited an absorption maximum of 521 nm. On the other hand, $HAuCl_4$ has an absorption peak at 442 nm, this peak is not due to the LSPR phenomenon. Instead, it arises from electronic transitions within the $HAuCl_4$ molecular complex. LSPR is a property of metallic nanoparticles, not ionic or molecular species like $HAuCl_4$. The surface plasmon resonance (SPR) phenomenon refers to the oscillation of unbound electrons on the outside of a solid substance. Metal nanoparticles provide support for the localized surface plasmon resonance (LSPR). The localized surface plasmon resonance (LSPR) takes place when the frequency of incoming light aligns with the inherent frequency of electrons on the surface.[37,38] The absorption intensity and wavelength are correlated with physical characteristics of AuNPs, such as their structure, shape, metal composition, and size.[37,39,40] The synthesised spherical AuNPs with a diameter of approximately 20 nm had surface plasmon band peaks at 521 nm in the LSPR spectrum. The wavelength shifts to higher values with

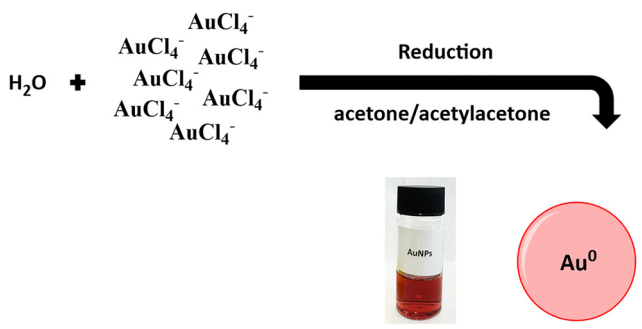

Scheme 1 Schematic representation of the synthesis of gold nanoparticles during the process.

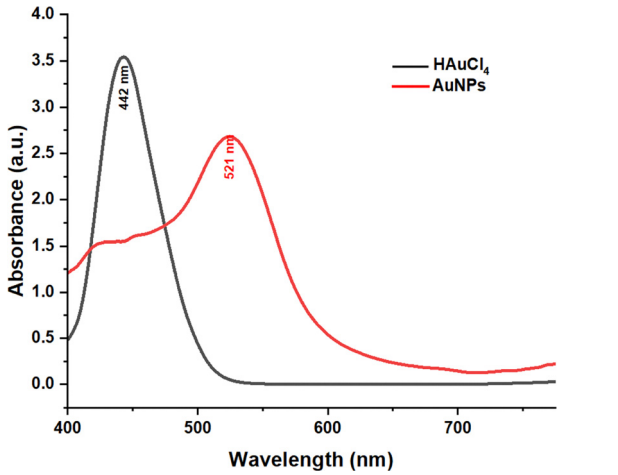

Fig. 2 LSPR absorption spectrum of hydrogen tetrachloroaurate (gold ions) and gold nanoparticles.

an increase in the nanoparticle's diameter, as depicted in (Table S2).

Transmission electron microscopy (TEM) is used to measure the size and examine the surface structure of nanoparticles, making them ideal for analysing the structural and chemical properties of nanomaterials at the nanoscale Transmission electron microscopes have a maximum magnification of 50 million times, allowing for clear observation of small details.[41] In the present study, the morphology and optical properties of the synthesised gold nanoparticles were directly influenced by the change in the percentage of the reducing agent. The most favourable characteristics of gold nanoparticles were obtained at higher concentration, corresponding to a 1 mL quantity of the reducing agent. The TEM images of Au NPs revealed the size of Au NPs in the range of 13 to 17 nm, which was measured by ImageJ software. TEM images indicated that most of the formed nanoparticles are spherically shaped (Fig. 3).

The technique of dynamic light scattering was used to assess the mean size, size distribution, and possible aggregation of the synthesized gold nanoparticles (AuNPs).[42,43] The most favourable characteristics of gold nanoparticles including stability, tuneable size and shape, surface modifiability, biocompatibility, strong optical and catalytic properties, and ease of production, were obtained at a higher concentration, corresponding to 1 mL quantity of RA. This was determined through a systematic modulation in the concentration of the reducing agent. The size distribution was very narrow at this concentration, with an average particle diameter of approximately 20 nm, as confirmed by TEM analysis. In addition, only one peak was observed in the graph, indicating that there were no particles of very different sizes in the colloid.[44] PDI quantifies the level of "non-uniformity" in a distribution. This value was determined using the width of the size distribution. The range spans from zero, representing a perfectly uniform sample, to 1.0, indicating a substantially polydisperse sample with different particle sizes.[42,43] A broad particle size distribution profile is denoted by PDI values greater than 0.7.[45,46] The PDI value of 0.263 indicates a monodisperse colloidal system with reliable stability, consistent with the benchmark that PDI $<$ 0.3 reflects high-quality nanoparticle dispersions. Compared with citrate-

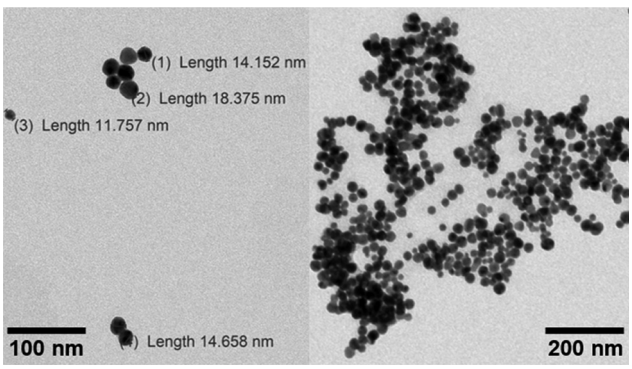

Fig. 3 TEM images of gold nanoparticles at 100 and 200 nm scales. Inset: particle size distribution histogram derived from ImageJ analysis of $>$200 particles, confirming narrow distribution around 14–17 nm.

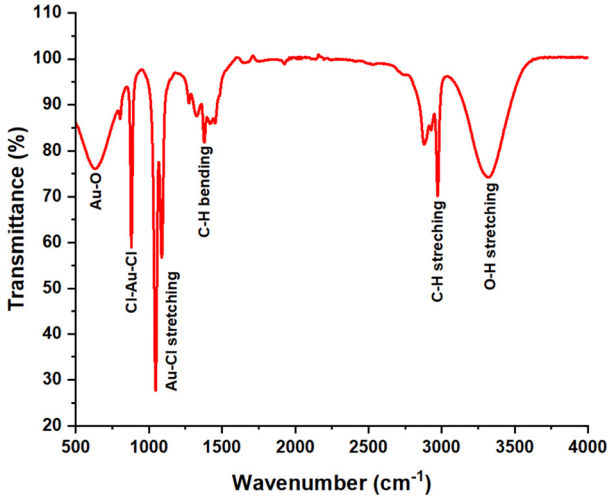

Fig. 4 FTIR spectra of gold nanoparticles.

and ascorbic acid- mediated reduction, which frequently yield broader or polydisperse size distribution requiring further optimisation,[15,18,19] the acetone- acetylacetone protocol consistently produces AuNPs with lower PDI value and enhanced reproducibility. Generally, an increase in the concentration of the reducing agent results in a more rapid progression of the kinetics of the reduction reaction, which ultimately causes the particle size to decrease. This is because a greater concentration of reducing agent can facilitate the nucleation and development of smaller nanoparticles by providing more electrons to reduce the gold ions. The average size of gold nanoparticles synthesized using varying concentrations of the reducing agent, as determined by DLS and TEM, is shown in (Table S2). The $\pm$ values reported for TEM, DLS, and PDI measurements correspond to the standard deviation of three independent replicates, unless otherwise specified.[47]

The FTIR is an exceptionally sensitive technology used to identify the specific functional group existing between the reducing agent and gold precursor. The identification of each functional group in nanoparticle suspensions may be achieved by analyzing the change in peaks. FTIR spectroscopy provides evidence of the functionalization of AuNPs by showing the interactions between the AuNPs and the agent used for functionalization.[48] Fig. 4 shows the FTIR spectra of AuNPs, compared with $HAuCl_4$, show distinct stretching and bending modes at 3321, 2971, 1375, 1087, 1046, 879, and 626 cm^{-1}, corresponding to Au–Cl, Cl–Au–Cl, and Au–O interactions. In summary, the FTIR spectra of gold nanoparticles are distinct from those of gold ions due to differences in their chemical environments, surface chemistry, aggregation states, ligand interactions, and physical properties like size and shape. These factors collectively contribute to the unique vibrational signatures observed in the FTIR spectra of gold nanoparticles.

4. Conclusion

This paper demonstrates the synthesis of gold nanoparticles using an improved protocol and **the** optimized composition of

the reducing reagent. This process involves the reduction of $HAuCl_4$ using acetone/acetylacetone as a reducing agent at room temperature. A red solution was obtained, indicating the formation of AuNPs. Herein, it was chosen the best outcome for gold nanoparticles with 1 mL of reducing agent (acetone and acetylacetone) present in a ratio of 1 : 2. The absorption band of 521 nm constituted the surface plasmon resonance (SPR) of the AuNPs. The TEM images of AuNPs reveal that the particles are predominantly spherical and have an average dimension of 14.7 ± 2.4 nm. The average particle size determined by DLS was 23.7 ± 1.7 nm, with a corresponding polydispersity index (PDI) of 0.263. AuNPs were synthesized using a simple and rapid method. The resulting spherical and small particles with ease of surface functionalization and stability can be used for a variety of diagnostic applications.

Author contributions

Vian Mahmood Saleh: investigation, analysis, writing, review and editing. Chris Zaleski: methodology, supervision. Sergey A. Piletsky: conceptualisation, methodology. Elena Piletska: supervision, writing, review and editing.

Conflicts of interest

There are no conflicts of interest to declare.

Data availability

The data supporting this article have been included as a part of the supplementary information (SI). Supplementary information is available. See DOI: **https://doi.org/10.1039/d5nj03249k**.

Acknowledgements

The authors express gratitude for the doctoral scholarship from The Higher Committee of Education and Development in Iraq (HCED) awarded to V. M. S. Additionally, the authors gratefully acknowledge the University of Leicester Core Biotechnology Services Electron Microscopy Facility and Natalie S. Allcock for their support in producing TEM images of gold nanoparticles.

Notes and references

1 M. Faraday, *SPIE Milestone Series*, 1996, **120**, 9–27.
2 J. E. Hutchison, *ACS Nano*, 2008, **2**, 395–402.
3 M.-C. Daniel and D. Astruc, *Chem. Rev.*, 2004, **104**, 293–346.
4 L. Dykman and N. Khlebtsov, *Chem. Soc. Rev.*, 2012, **41**, 2256–2282.
5 P. K. Jain, X. Huang, I. H. El-Sayed and M. A. El-Sayed, *Plasmonics*, 2007, **2**, 107–118.
6 Z. Wang, X. Sun, Y. Xu, L. Yang, M. Wang, Y. Xia, Y. Wang, Y. Tang, C. Qiao and Y. Lin, *Colloids Surf., A*, 2024, **696**, 134292.
7 D. A. Giljohann and C. A. Mirkin, *Nature*, 2009, **462**, 461–464.
8 X. Huang, P. K. Jain, I. H. El-Sayed and M. A. El-Sayed, *Nanomedicine*, 2007, **2**, 681–693.
9 E. Boisselier and D. Astruc, *Chem. Soc. Rev.*, 2009, **38**, 1759–1782.
10 C. N. R. Rao, A. Müller and A. K. Cheetham, *The chemistry of nanomaterials: synthesis, properties and applications*, John Wiley & Sons, 2006.
11 A. H. Lu, E. e L. Salabas and F. Schüth, *Angew. Chem., Int. Ed.*, 2007, **46**, 1222–1244.
12 Y. Xia, P. Yang, Y. Sun, Y. Wu, B. Mayers, B. Gates, Y. Yin, F. Kim and H. Yan, *Adv. Mater.*, 2003, **15**, 353–389.
13 C. Burda, X. Chen, R. Narayanan and M. A. El-Sayed, *Chem. Rev.*, 2005, **105**, 1025–1102.
14 K. B. Narayanan and N. Sakthivel, *Adv. Colloid Interface Sci.*, 2010, **156**, 1–13.
15 S. Ahmed, M. Ahmad, B. L. Swami and S. Ikram, *J. Adv. Res.*, 2016, **7**, 17–28.
16 S. Iravani, *Green Chem.*, 2011, **13**, 2638–2650.
17 P. Raveendran, J. Fu and S. L. Wallen, *J. Am. Chem. Soc.*, 2003, **125**, 13940–13941.
18 J. Turkevich, P. C. Stevenson and J. Hillier, *Discuss. Faraday Soc.*, 1951, **11**, 55–75.
19 G. Frens, *Nat. Phys. Sci.*, 1973, **241**, 20–22.
20 C. Deraedt, L. Salmon, S. Gatard, R. Ciganda, R. Hernandez, J. Ruiz and D. Astruc, *Chem. Commun.*, 2014, **50**, 14194–14196.
21 S. Kundu, A. Pal, S. K. Ghosh, S. Nath, S. Panigrahi, S. Praharaj and T. Pal, *Inorg. Chem.*, 2004, **43**, 5489–5491.
22 L. Chen, X. Wang, W. Lu, X. Wu and J. Li, *Chem. Soc. Rev.*, 2016, **45**, 2137–2211.
23 S. A. F. Kusuma, J. A. Harmonis, R. Pratiwi and A. N. Hasanah, *Sensors*, 2023, **23**, 8172.
24 K. Qian, C. Yao, Y. Wang, Q. Yang, S. Xiang, Q. Pei, T. Zhu, H. Liu and S. Dong, *IEEE Trans. Biomed. Eng.*, 2025, **72**, 3233–3243.
25 Y. Lei, S. Dong, R. Liang, S. Xiang, Q. Huang, J. Ma, H. Kou, L. Yu and C. Yao, *IEEE Trans. Biomed. Circ. Syst.*, 2025, **19**, 496–510.
26 J. Sun, X. Yu, W. Li, B. Jia, D. Shi, Y. Song, F. Wang, B. Cao and C. Jiang, *Sens. Actuators, B*, 2025, **433**, 137422.
27 C. Gao, H. Sun and J. Du, *Angew. Chem., Int. Ed.*, 2025, **64**, e202420079.
28 Y. Gao, Y. Wang, J. Jiang, P. Wei and H. Sun, *Small*, 2025, **21**, 2411432.
29 A. Shah, S. Akhtar, F. Mahmood, S. Urooj, A. B. Siddique, M. I. Irfan, M. Naeem-ul-Hassan, M. Sher, A. Alhoshani and A. Rauf, *Surf. Interfaces*, 2024, **51**, 104556.
30 M. Awan, S. Rauf, A. Abbas, M. H. Nawaz, C. Yang, S. A. Shahid, N. Amin and A. Hayat, *J. Mol. Liq.*, 2020, **317**, 114014.
31 B. Chaudhuri and S. Raychaudhuri, *IVD Technol.*, 2001, **7**, 46–54.
32 M. Bindhu and M. Umadevi, *Spectrochim. Acta, Part A*, 2014, **128**, 37–45.

33 N. Leopold and B. Lendl, *J. Phys. Chem. B*, 2003, **107**, 5723–5727.
34 I. Hammami and N. M. Alabdallah, *J. King Saud Univ., Sci.*, 2021, **33**, 101560.
35 M. Danaei, M. Dehghankhold, S. Ataei, F. Hasanzadeh Davarani, R. Javanmard, A. Dokhani, S. Khorasani and Y. M. Mozafari, *Pharmaceutics*, 2018, **10**, 57.
36 S. Mourdikoudis, R. M. Pallares and N. T. Thanh, *Nanoscale*, 2018, **10**, 12871–12934.
37 J. Jana, M. Ganguly and T. Pal, *RSC Adv.*, 2016, **6**, 86174–86211.
38 A. R. Sadrolhosseini, A. Noor, M. M. Moksin and K. Y. Kim, *Plsmonics-Principles and Applications*, 2012, pp. 253–282.
39 D. Sevenler, N. L. Ünlü and M. S. Ünlü, *Nanobiosensors Nanobioanal.*, 2015, 81–95.
40 K. Thomas, *Nanomater. Chem.*, 2007, 185–218.
41 T. Patil, R. Gambhir, A. Vibhute and A. P. Tiwari, *J. Cluster Sci.*, 2023, **34**, 705–725.
42 M. Danaei, M. Dehghankhold, S. Ataei, F. Hasanzadeh Davarani, R. Javanmard, A. Dokhani, S. Khorasani and M. Mozafari, *Pharmaceutics*, 2018, **10**, 57.
43 Y. Gao, M. Arokia Vijaya Anand, V. Ramachandran, V. Karthikkumar, V. Shalini, S. Vijayalakshmi and D. Ernest, *J. Cluster Sci.*, 2019, **30**, 937–946.
44 S. Banerjee, A. K. Saha, B. Show, J. Ganguly, R. Bhattacharyay, S. K. Datta, H. Saha and N. Mukherjee, *RSC Adv.*, 2015, **5**, 5667–5673.
45 E. Joseph and G. Singhvi, *Nanomater. Drug Delivery Ther.*, 2019, 91–116.
46 T. Mudalige, H. Qu, D. Van Haute, S. M. Ansar, A. Paredes and T. Ingle, *Nanomater. Agri-Food Appl.*, 2019, 313–353.
47 I. Montes-Burgos, D. Walczyk, P. Hole, J. Smith, I. Lynch and K. Dawson, *J. Nanopart. Res.*, 2010, **12**, 47–53.
48 V. K. T. Ngo, D. G. Nguyen, T. P. Huynh and Q. V. Lam, *Adv. Nat. Sci.: Nanosci. Nanotechnol.*, 2016, **7**, 035016.

